In-line liquid-crystal microcell polarimeter for high-speed polarization analysis

Bharat R. Acharya, C. K. Madsen, K. W. Baldwin, R. A. MacHarrie, and J. A. Rogers

Bell Laboratories, Lucent Technologies, Murray Hill, New Jersey 07974

L. Möller

Bell Laboratories, Lucent Technologies, Holmdel, New Jersey 07733

C. C. Huang

School of Physics and Astronomy, University of Minnesota, Minneapolis, Minnesota 55455

R. Pindak

National Synchrotron Light Source, Brookhaven National Laboratory, Upton, New York 11973

Received December 23, 2002

We report a type of high-speed microcell polarimeter that utilizes microelectrodes, liquid-crystal films, and ultrathin high-contrast polarizers, all integrated between the tips of two optical fibers. When combined with optimized nematic liquid-crystal materials, this compact (2.5 cm × 0.5 cm × 0.5 cm) device offers excellent optical properties and continuous, high-speed operation at >2 kHz with moderately low operating voltages. It requires no bulk optical elements, and it shows excellent performance when implemented for the measurement of degree of polarization in 10-Gbit/s test systems. Polarimeters based on this design have promising potential applications in polarization analysis for high-speed optical communication systems.

OCIS codes: 060.0060, 160.3710, 230.3720.

With the recent increase in the data transmission rate, analysis of the state of polarization (SOP) will become a required, basic feature of advanced optical communication systems. Polarimeters that are suitable for practical optical network applications must satisfy many challenging requirements, including high speed, low loss, and low-power operation at low cost. One attractive class of polarimeter design uses a rotating wave plate and a polarizer architecture with a single detector.[1,2] This design is attractive in part because it requires only one detector and it avoids errors associated with the gain mismatch in a multidetector system.[3] Many of the existing components for these technologies, such as lithium niobate waveguides, piezoelectric fiber squeezers, electro-optic ceramic elements, nematic liquid crystals (NLCs), have some combination of disadvantages that include high cost, high insertion loss, high operating voltages, and low-speed operation. NLC-based devices have important attractive features: they have a strong potential to be low in cost and they have high electro-optic modulation and low-power, nonmechanical operation. They are also easy to fabricate, and they can have low insertion loss. However, until recently,[4] because of long switching times (~10 ms, which corresponds to a rotational frequency of ~12 Hz) the high-speed operation (of the order of kilohertz) that is necessary for most interesting network applications was not demonstrated with these systems. In this Letter we report a class of high-speed NLC-based microcell polarimeters that are formed directly between the tips of two optical fibers. These devices offer low insertion loss in a compact (2.5 cm × 0.5 cm × 0.5 cm including the mounts) fiber-based device that requires no bulk optics. With optimized design and NLC materials, an acquisition time of ~250 μs is possible at moderately low operating voltages. These polarimeters have been implemented for degree-of-polarization (DOP) and SOP measurements in 10-Gbit/s transmission systems.

We begin the fabrication of these microcell polarimeters by gluing an ~30-μm-thick Polarcor Ultrathin (Corning, Inc.) polarizer onto the tip of an optical fiber that is mounted in a glass ferrule assembly. Four ~0.2-μm-thick electrodes are then micropatterned directly onto the surface of the polarizer such that the core of the optical fiber is aligned at the center. To achieve a strong and uniform electric field across the core we make the electrodes ~5 μm wide and separate them by ~25 μm. Another identical fiber ferrule assembly, without a polarizer, is micropatterned with similar integrated electrodes and is actively aligned to the other ferrule with a predetermined gap of ~4 μm between them set by the diameters of short glass fiber spacers. To provide access to the electrodes on the ferrule facets we rotate the second ferrule by 90° with respect to the first. Figure 1 shows the configuration of the microcell polarimeter. Loading the NLC (Merck Chemicals MLC-14200-000) by capillary action into the narrow space between the two ferrules completes the fabrication of the microcell polarimeter. For this NLC material the 4-μm-thick

0146-9592/03/131096-03$15.00/0

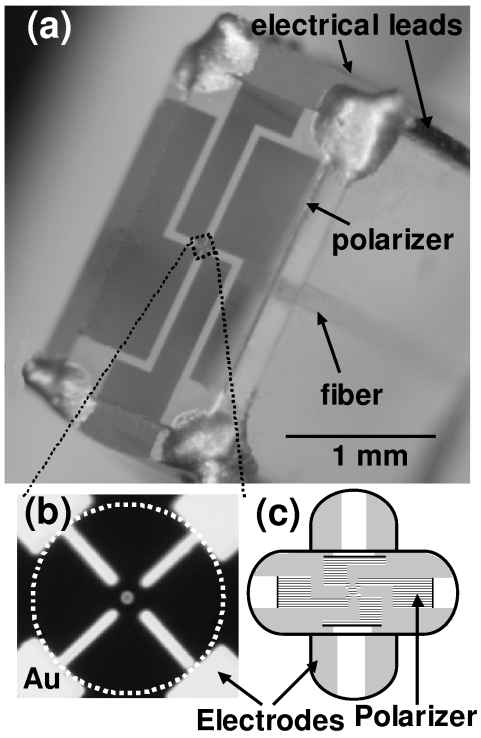

Fig. 1. Configuration of the polarimeter: (a) Fiber ferrule assembly with Polarcor Ultrathin polarizer. (b) Electrode structure. Dotted curve, perimeter of the 125-μm-diameter fiber; dot at the center, core of the fiber. (c) Cross-sectional view of the polarimeter after two ferrules are assembled together.

aligned layer renders a phase difference of ~90° between ordinary and extraordinary rays. To control the azimuthal orientation (ϕ) of the optic axis of the NLC we connect the electrodes that face each other on the opposite ferrules and apply a 10-kHz square-wave potential with 200-V peak amplitude modulated by $\sin(i \times 90 + \phi)$ to the ith electrode. For these high fields, any possible misalignment of the director at the thin liquid crystal–glass interface has a negligible effect on the overall alignment of the director. As a result, alignment layers are not needed.

Placing the device between a laser source at 1.55 μm and a polarization controller (PolCon) such that the optical signal passes first through the polarizer and then through the NLC layer provides a means to characterize the device's performance. The signal from the PolCon enters a polarization analyzer. The optic axis of the NLC layer is aligned at 45° with respect to the transmission axis of the polarizer by adjustment of the potentials applied to the electrodes. The PolCon is then adjusted to yield right-circularly polarized light at the polarization analyzer, thereby canceling any transformation of the SOP caused by the length of the fiber between the NLC layer and the detector. The polarization analyzer monitors the evolution of the SOP on the Poincaré sphere as the optic axis of the polarizer rotates. Figure 2(a) shows the evolution of the SOP on the Poincaré sphere when the optic axis of the NLC layer is rotated through 180° by rotation of the electric field. An almost perfect figure-8 contour indicates that the NLC microcell wave plate behaves as a quarter-wave plate (QWP).[2] Inserting an analyzer between the QWP and the detector and measuring the intensity of the signal at the photodetector behind it give a quantitative measure of the phase retardation of the QWP. With the optic axis aligned parallel to the transmission axis of the polarizer, the PolCon is adjusted until the intensity at the detector is minimum, and then the optic axis of the wave plate is rotated to permit us to monitor the variation in the optical intensity. The theoretical fit to the experimental intensity profile as a function of rotation angle yields a phase retardation of 91° ± 0.6° for the NLC microcell QWP.

To determine the maximum distortion-free speed of rotation of the QWP we rotate its optic axis by applying a sinusoidal voltage with $V_0 = 200$ V peak amplitude with a variable frequency. Until a 2-kHz rotational speed is reached, the modulation of the linearly polarized light is uniform in time and the modulation depth is constant. As the rotational speed of the field exceeds 2.5 kHz the NLC director can no longer follow the applied electric field, and defects in the director field begin to appear. This behavior results in decreased transmission, asymmetric modulation, and reduced modulation depth. Figure 2(b) depicts the variation of the modulation depth as a function of the applied frequency. It is clear from the figure that the NLC QWP is capable of achieving more than 2-kHz rotational speed. At an elevated temperature of 75 °C the NLC material acquires optimum speed, and similar switching performance can be achieved even at the lower peak amplitude voltage of $V_0 = 100$ V.[4] However, the thickness of the LC layer has to be optimized to compensate for the decrease in the optical retardation at these elevated temperatures.

We test the performance of the polarimeter for quantitative measurement of degree of polarization by launching light at 1.55 μm such that it passes through the QWP and then the polarizer and rotating the QWP. Let $\mathbf{S} = [S_0, S_1, S_2, S_3]^{\mathrm{T}}$ be the Stokes vector of the incident light at the input of the polarimeter

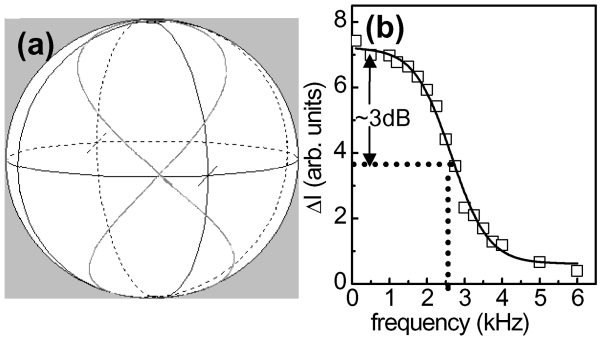

Fig. 2. (a) Evolution of the SOP of linearly polarized light on the Poincaré sphere when the optic axis of the quarter-wave plate is rotated through 180°. The linearly polarized state (at the equator) gradually evolves to the left- (at the south pole) and the right- (at the north pole) circularly polarized states with elliptically polarized states between them. The slight asymmetry is due to imperfect subtraction of the effect of the fiber. (b) Modulation depth (ΔI) as a function of the rotational frequency of the optic axis of the polarimeter. The solid curve is a guide to the eye.

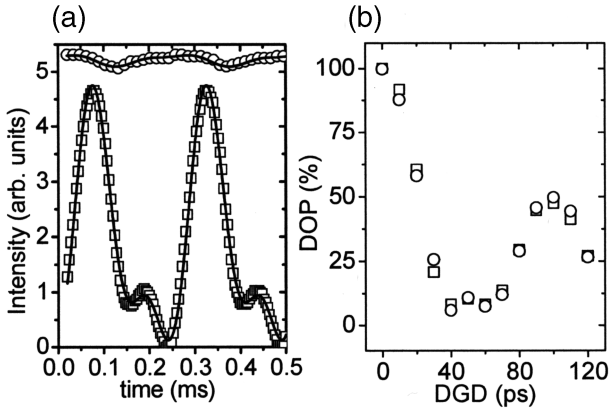

Fig. 3. (a) Variation of intensity as a function of time for polarized (□) and unpolarized (○) light. (b) Variation of the degree of polarization as a function of the DGD as measured by a NLC polarimeter (□) and a conventional polarization analyzer (○).

(i.e., at the fiber–NLC interface), where T represents the transpose. If the optic axis of the QWP rotates continuously with frequency ω, the intensity of the light at the detector at time t consists of a truncated Fourier series with second and fourth harmonics and is given by[5]

$$I(t) = \frac{1}{2}\left[\left(S_0 + \frac{S_1}{2}\right) + S_3 \cos 2\omega t + \frac{S_1}{2}\cos 4\omega t + \frac{S_2}{2}\sin 4\omega t\right]. \quad (1)$$

And the DOP is defined as $(S_1^2 + S_2^2 + S_3^2)^{1/2}/S_0$. Thus, by monitoring the transmitted intensity as a function of time, we can determine the Stokes parameters of the incident beam in the polarizer frame of reference. By evaluating the transformation/calibration matrix, which takes into account the transformation introduced by coordinate rotation and the length of the optical fiber between the SOP generator and the fiber–NLC interface, we can determine the SOP in the laboratory frame of reference.[6,7] Inasmuch as the DOP is invariant during these transformations, we can use these Stokes parameters in the polarizer frame of reference to calculate the DOP of the signal.

To measure the DOP we first filter an optical signal from an amplified stimulated emission source at 1.55 μm and then launch it through the NLC microcell polarimeter such that it passes through the QWP and then the polarizer. We rotate the optic axis of the QWP by applying a sinusoidal voltage with $V_0 = 200$ V peak amplitude at 2 kHz. A photodetector monitors the optical intensity as a function of time for nominally unpolarized and polarized input light (generated by insertion of a polarizer between the filter and the polarimeter). Figure 3(a) depicts the intensity variation as a function of time during rotation of the QWP. For the nominally unpolarized light, a small ripple observed in the intensity indicates a slight polarization, as we confirmed by rotating a polarizer between the source and the detector. Theoretical fits to the experimental data yield the values for the Stokes parameters in the polarizer frame of reference at the fiber NLC–QWP interface. The measured DOPs for the nominally unpolarized and polarized light were 0.02 and 1.03, respectively.

To illustrate a specific potential application for this polarimeter, we implemented it to measure the DOP in a 10-Gbit/s optical transmission system that was subjected to various amounts of polarization mode dispersion. A 33% return-to-zero signal was launched to a PolCon and then to a polarization mode dispersion emulator with a tunable differential group-delay (DGD) element. The signal was split into two equal halves by a 3-dB splitter. One half of the optical signal went to the NLC polarimeter and the other half to a Hewlett–Packard (HP) polarization analyzer. We then introduced different amounts of DGDs by adjusting the tunable element and measured the corresponding DOPs simultaneously, using a conventional polarization analyzer (HP 8509B with a DOP accuracy of $\pm 2.5\%$) and the NLC polarimeter. Figure 3(b) shows the variation of the DOP as a function of DGD as measured by the NLC polarimeter against the conventional polarimeter. Clearly, the DOP values measured by the NLC microcell polarimeter agree well with those measured by the HP polarization analyzer.

In this Letter we have introduced a new type of high-speed in-line nematic liquid-crystal microcell polarimeter that is fabricated directly between the tips of two optical fibers. These devices have been used for measurements of state of polarization in tests of 10-Gbit/s systems, and close agreement between the results from a commercially available polarimeter and from the device described here was observed. Although the insertion loss in the current device is ~6 dB (including 3 dB from the polarizer) it can be reduced significantly by improved alignment and packaging [the theoretical minimum loss between two fibers separated by a 4-μm-thick NLC layer is ~0.05 dB (Ref. 8)]. Simple fabrication, low cost, compact design, and good optical properties of these devices suggest that they have potential applications for high-speed polarization analysis in optical networks.

This study was partly supported by a National Science Foundation Grant Opportunities for Academic Liaison with Industry grant.

References

1. E. Collet, Opt. Commun. **52,** 77 (1984).
2. R. M. A. Azzam, J. Opt. Soc. Am. A **17,** 2105 (2000).
3. P. Williams, Appl. Opt. **38,** 6508 (1999).
4. B. R. Acharya, K. W. Baldwin, R. A. MacHarrie, C. C. Huang, R. Pindak, and J. A. Rogers, Appl. Phys. Lett. **81,** 5243 (2002).
5. E. Collet, in *Polarized Light: Fundamental and Applications* (Marcel Dekker, New York, 1990), p. 103.
6. P. Olivard, P. Y. Gerligand, B. Le Jeune, and J. Lotrian, J. Phys. D **32,** 1618 (1999).
7. R. M. A. Azzam, Opt. Lett. **12,** 558 (1987).
8. L. Dupont, J. L. de Bougrenet de la Tocnaye, M. L. Gall, and D. Penninckx, Opt. Commun. **176,** 113 (2000).